Energy & Environmental Science

Cite this: *Energy Environ. Sci.*, 2012, **5**, 9021

www.rsc.org/ees

PAPER

CO_2 capture from gas stream by zeolite 13X using a dual-column temperature/vacuum swing adsorption†

Fengsheng Su and Chungsying Lu*

Received 1st November 2011, Accepted 6th August 2012
DOI: 10.1039/c2ee22647b

A dual-column temperature/vacuum swing adsorption (TVSA) with zeolite 13X was built to study cyclic CO_2 capture from a gas stream. The adsorption capacities and the physicochemical properties of 13X were preserved through 100 cycles of adsorption–desorption operation, displaying the stability of 13X for cyclic TVSA. The desorbed CO_2 concentration could reach above 90%, which is practical for further utilization or permanent storage. The heat input required to regenerate spent 13X was low, reflecting an energy-efficient CO_2 adsorbent. A statistical analysis on the adsorbent cost of CO_2 capture revealed that the 13X could be cost-effective after extensive TVSA cycling. 13X showed less moisture sensitivity below 30 °C and showed a stable adsorption performance for CO_2 under humid conditions. These results suggest that a dual-column TVSA with solid 13X is has the possibility to be a promising CO_2 capture technology.

1. Introduction

The use of CO_2 capture, utilization and storage (CCUS) technologies on flue gas is considered to be a useful method of lessening global warning.[1] Several post-combustion CO_2 capture technologies including absorption, adsorption, cryogenics, membranes and so forth, have been studied.[2,3] Among them, the design of a full-scale adsorption–desorption operation with solid adsorbents for cyclic CO_2 capture might be feasible. Therefore, the development of a promising material that would adsorb CO_2 with a high working capacity and the ability to be regenerated with a low energy input will undoubtedly enhance the competitiveness of an adsorptive separation system in flue gas applications.[4,5]

The adsorption–desorption operation for cyclic CO_2 capture was commonly conducted by means of pressure swing adsorption (PSA), vacuum swing adsorption (VSA), or temperature swing adsorption (TSA) with many kinds of low-temperature solid adsorbents. These solid adsorbents include carbon based adsorbents[6–10] and zeolite based adsorbents.[11–23]

A combination of TSA and VSA (TVSA) was found to reduce significantly the desorption time of CO_2 from the spent amine-loaded carbon nanotubes[9] and spherical mesoporous silica particles[24] as compared to TSA or VSA. The productivity and purity of desorbed CO_2 with activated carbon followed the order TVSA > VSA > TSA and the influent CO_2 could be concentrated to 97% by TVSA operation.[25] The International Energy Agency (IEA) reported that the TVSA system would be more energy efficient if the adsorption process was conducted at moderate temperature (~125 °C) or high temperature (~325 °C).[26] It was concluded that the TVSA system with a promising solid adsorbent would possibly be energy efficient with a high purity of desorbed CO_2. However, such information in terms of working capacity, cycle time, desorbed CO_2 concentration level, and multi-cycle durability is still very limited in the literature.

This article therefore studied cyclic CO_2 adsorption with 13X, which possess a high CO_2 adsorption capacity,[13] *via* dual-column TVSA. The heat input required to regenerate spent 13X was determined and compared with that of a rich CO_2–30% monoethanolamine (MEA) mixture, which has been recognized as the most mature CO_2 capture process so far.[2] A statistical analysis of the cost of cyclic CO_2 adsorption and the moisture effect on CO_2 adsorption of 13X was also conducted to evaluate their practicability in flue gas treatment.

2. Materials and methods

2.1 Adsorbents

Commercially available zeolite 13X (UOP LLC, Des Plaines, IL) with a Si/Al molar ratio of 2–3 and a mass density of 0.61 g cm^{-3} was selected as the adsorbent for cyclic CO_2 capture because of its wide use in gas separation applications. Before adsorption tests, the 13X was pretreated at 100 °C for 2 h in an oven to remove adsorbed moisture.

2.2 Adsorption experiments

The experimental setup for cyclic CO_2 adsorption on 13X *via* a dual-column TVSA system is shown in Fig. 1. The column was

Department of Environmental Engineering, National Chung Hsing University, Taichung 40227, Taiwan. E-mail: clu@nchu.edu.tw; Fax: +886-4-22862587; Tel: +886-4-22852483

† This article was submitted as part of a Themed Issue on carbon dioxide. Other papers on this topic can be found in issue 6 of vol. 5 (2012).

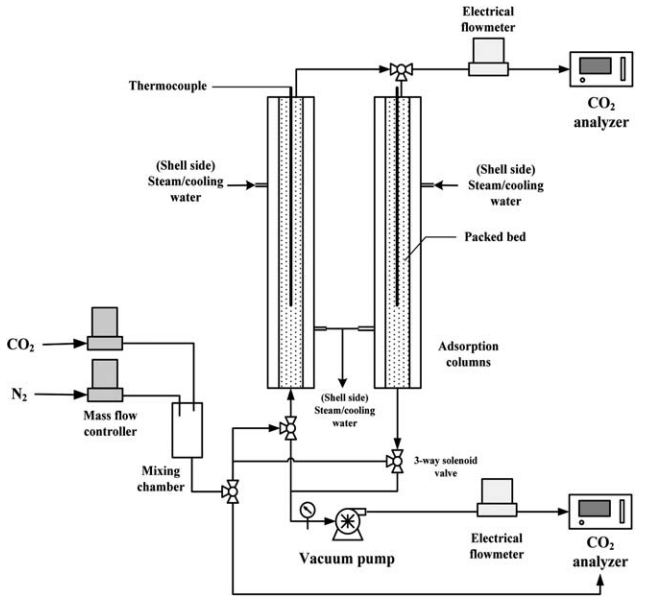

Fig. 1 Schematic diagram of a dual-column TVSA system for cyclic CO_2 capture from gas stream.

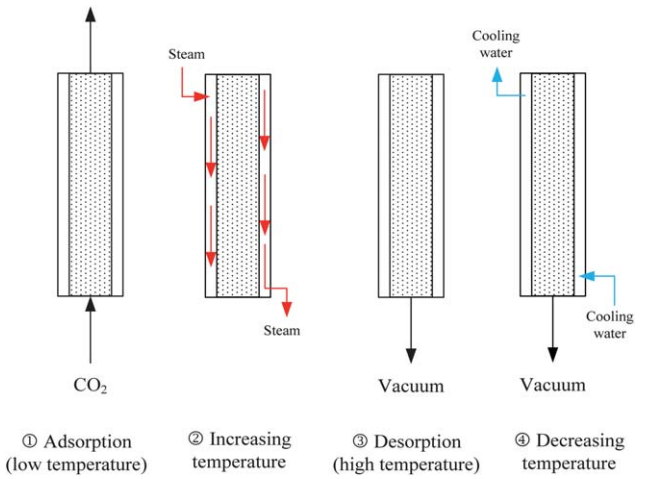

Fig. 2 Four-step operation of TVSA system.

made of stainless steel with a total height of 30 cm and an internal diameter of 2.2 cm, and filled with 15 g of 13X, equivalent to a packing height of 6 cm. The column contained an inner column and shell which was designed to pass through the steam fluid or the cooling water to increase or decrease the temperature of the inner column, respectively. Two mass flow controllers (MKS Instruments Inc., Andover, MA) were employed to control the influent CO_2 concentration by regulating the flow rates of pure CO_2 (99.95%) and N_2 (diluting gas) entering the mixing chamber. The influent and effluent gas streams were flowed into a CO_2 analyzer for online measurement, and the associated concentrations (C_{in} and C_{eff}) were expressed in terms of percentage volume, which were converted to mg L^{-1} by the ideal gas law when the CO_2 adsorption capacity was calculated.

The C_{in} was set to 15%, which was selected to be representative of CO_2 concentrations in combustion gases from the coal-fired power plants (12–15%).[27] The influent flow rate (Q_{in}) was controlled at 0.1 L min^{-1}, equivalent to an empty-bed retention time of 13.6 s. The CO_2 adsorption capacity (q_t, mg g^{-1}) at a certain time (t, min) was estimated as

$$q_t = \frac{1}{m}\int_0^t (Q_{in}C_{in} - Q_{eff}C_{eff})\mathrm{d}t \quad (1)$$

where m is the weight of 13X (g) and Q_{eff} is the effluent flow rate (L min^{-1}). Integrating eqn (1) from $t = 0$ to t_b (breakthrough time when C_{eff} reaches 10% of C_{in}, that is, ≥90% CO_2 capture efficiency) gives the working CO_2 capacity (q_w, mg g^{-1}). Blank tests (without 13X) were also conducted. The q_t of blank was eliminated from the q_t of 13X.

2.3 Cyclic CO_2 adsorption experiments

The TVSA operation of each column contains four steps as shown in Fig. 2. The adsorption process was controlled at 25 °C and 1 bar as the first step. As the CO_2 adsorption reached a breakthrough, the adsorption process was switched to a heating process by inletting overheated steam fluid as the second step. The vacuum desorption started when the column temperature increased from the adsorption temperature to the desorption temperature as the third step. The vacuum pressure was controlled by the vacuum pump valve. Finally, the column was chilled down from the desorption temperature to the adsorption temperature by cooling water as the fourth step, and then the desorption process returned to the adsorption process. Cyclic CO_2 adsorption on 13X *via* TVSA operation was conducted for 100 cycles with two columns in parallel. While one column adsorbs at 25 °C and 1 bar, the other column desorbs at high temperature and low pressure, which must be predetermined by a laboratory test.

2.4 Analytical methods

CO_2 concentration was determined using a CO_2 analyzer (IR-208, Infrared Industries Inc., Hayward, CA). The physical properties of 13X were measured by N_2 adsorption/desorption at 77 K *via* a Micromeritics ASAP 2020 volumetric sorption analyzer (Norcross, GA). N_2 adsorption/desorption isotherms were analyzed at a relative pressure (P_{N_2}/P_0) range of 0.0001–0.99 and employed to determine surface area, pore volume and average pore diameter *via* the micropore (MP) method for pore sizes <1.7 nm and *via* the Barrett, Johner and Halenda (BJH) equation for pore sizes 1.7–300 nm.

The heat input required to regenerate spent 13X (regeneration heat, Q_{regen}) and the heat input required to heat 13X from the adsorption temperature to the desorption temperature (sensible heat, ΔH_s) were measured by a differential scanning calorimeter (DSC910, Instrument Specialists Inc., Twin Lakes, WI). The equilibrium amount of CO_2 desorption (q_{ed}) was determined by a thermogravimetric analyzer (TGA i1000, Instrument Specialists Inc., Twin Lakes, WI) when the thermodynamic properties of 13X regeneration was calculated.

The crystal phase of 13X before and after 100 cycles of TVSA operation was characterized by a powder X-ray diffractometer (XRD, Mac Science Co., Japan) using Cu Kα radiation (40 kV, 30 mA).

3. Results and discussion

3.1 Physical properties of 13X

Fig. 3 presents the N_2 adsorption/desorption isotherms of 13X. It is apparent that the adsorption isotherm exhibits a type II shape according to IUPAC classification,[28] with a rounded knee at a very low pressure (about 2 kPa) representing some micropores in 13X. After a very slow increase up to an absolute pressure of 80 kPa, the isotherm displays a fast increment with absolute pressure showing the mesoporous nature of 13X. A small closed adsorption/desorption hysteresis loop is also observed with an absolute pressure above 50 kPa, probably due to mesopores with a capillary condensation.

Fig. 4 shows the pore size distribution of 13X. It is evident that the micropores display a narrow size distribution mainly appearing in the pore size range of 0.3–0.5 nm, which is related to adsorption of CO_2 molecules (d_{CO_2} = 0.33 nm) on 13X.[29] The mesopores/macropores exhibit a broad size distribution but a small pore volume as compared to the micropores. Specific surface area, specific pore volume and average pore diameter respectively are 659.19 $m^2\ g^{-1}$, 0.238 $cm^3\ g^{-1}$, and 0.36 nm for pore sizes below 1.7 nm and 588.01 $m^2\ g^{-1}$, 0.314 $cm^3\ g^{-1}$, and 19 nm for pore size of 1.7–300 nm.

3.2 Desorption temperature and vacuum pressure

The employed desorption temperature (T_d) and vacuum pressure (P) were determined by a single-column TVSA system. Desorption experiments were conducted for 40 min to assure the achievement of desorption equilibrium. Fig. 5 shows the peak desorbed CO_2 concentration (C_{de}) profiles under various T_d. It is apparent that the C_{de} increased, but the time to reach desorption equilibrium decreased with a rise in T_d, which could be because that more CO_2 molecules were desorbed from spent 13X at a faster rate under a higher T_d. The C_{de} reached 55, 82 and 93% at T_d of 105, 130 and 140 °C, respectively. Thus, 140 °C was selected as T_d to determine P.

Fig. 6 shows the q_w during 10 cycles of TVSA operation (n) under various P. The AI was calculated based on the percentage ratio of q_w of regenerated 13X to the virgin one, thus 100% AI implies that the 13X has not deteriorated at all. It is evident that

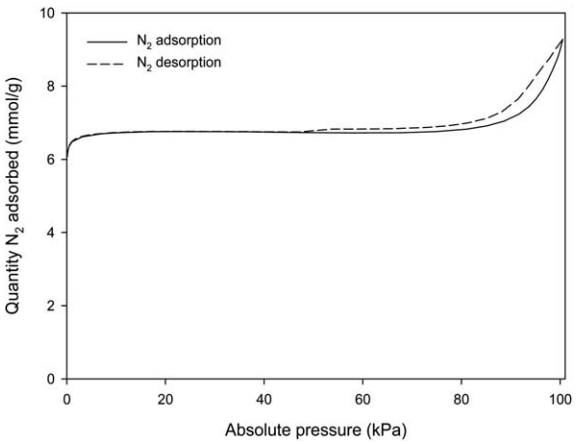

Fig. 3 N_2 adsorption and desorption isotherms of 13X.

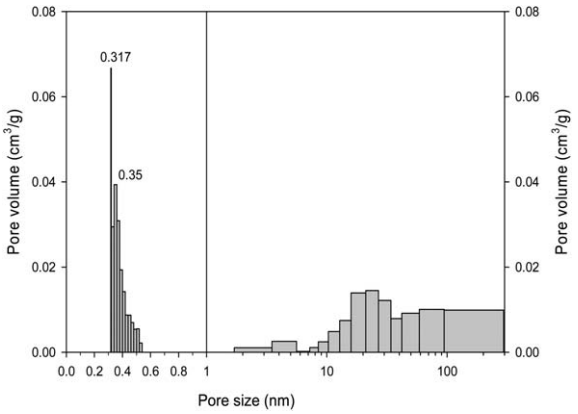

Fig. 4 Pore size distribution of 13X.

the q_w decreased with a rise in n and P. The q_w at $n = 1$, 2, and 10 are respectively 84.2, 83.1, and 82.3 mg g^{-1} corresponding to the AI of 100, 98.9, and 97.6% under P = 0.01 bar; 84.3, 79.5, and 76.9 mg g^{-1} corresponding to the AI of 100, 94.3, and 91.2% under P = 0.35 bar; 84.4, 76.3 and 68.1 mg g^{-1} corresponding to the AI of 100, 90.4, and 80.7% under P = 0.5 bar; and 84.1, 70.2, 65.1 mg g^{-1} corresponding to the AI of 100, 83.2, and 77.4% under P = 0.7 bar.

Although the q_w and AI appeared high under low P conditions (0.01 and 0.35 bar), it is very difficult to achieve such low P conditions in the large scale adsorber. The q_w and AI under P of 0.5 and 0.7 bar were close and preserved from n = 4 to 10. For practical purposes, a T_d of 140 °C and P of 0.7 bar were selected as desorption conditions in the cyclic CO_2 adsorption on 13X *via* a dual-column TVSA system.

3.3 Cyclic CO_2 adsorption on 13X

Fig. 7 shows the q_w and associated AI of 13X during 100 cycles of dual-column TVSA operation. The reported q_w and AI of each cycle were the mean values of the two columns. The average t_b of each column after n = 3 is around 30 min while the time to increase temperature from 25 to 140 °C and to decrease

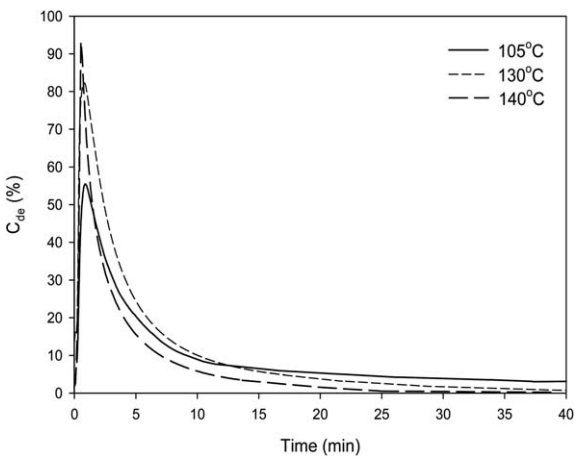

Fig. 5 Effects of desorption temperature on the effluent CO_2 concentration.

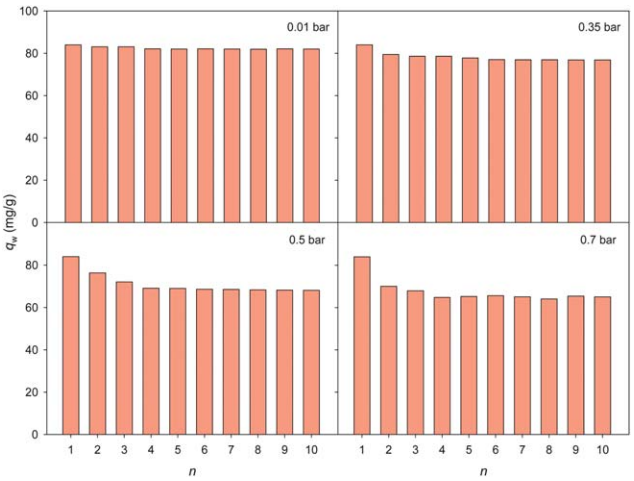

Fig. 6 Effects of vacuum pressure on the working CO_2 capacity.

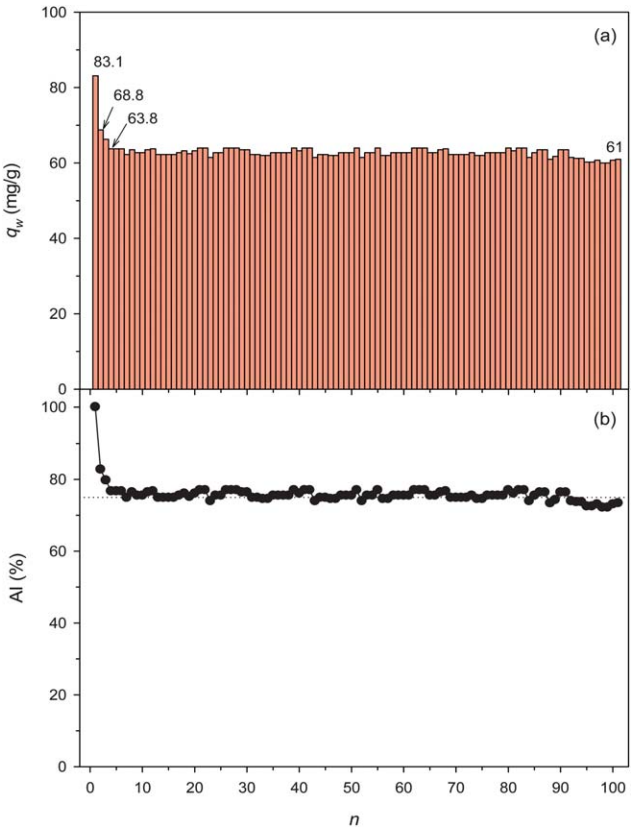

Fig. 7 Adsorption performance of CO_2 during 100 cycles of dual-column TVSA operation.

temperature from 140 to 25 °C are 12 and 8 min, respectively. The desorption time of each column is thus approximately 10 min.

The q_w at $n = 1$, 2, 4, 50 and 100 are respectively 83.1, 68.8, 63.8, 62.7 and 61 mg g^{-1} corresponding to AI of 100, 82.8, 76.8, 75.5 and 73.4%. The q_w decreased from 83.1 to 63.8 mg g^{-1} while the AI decreased from 100 to 76.8% after the third cycle of TVSA operation. The attrition of q_w could be explained by the use of practical desorption conditions instead of efficient desorption conditions. However, the q_w and AI appeared rather stable and showed 2.8 mg g^{-1} and 3.4% attrition from $n = 4$ to 100, respectively. This reveals that the 13X could be stably employed in the prolonged cyclic CO_2 capture *via* a dual-column TVSA operation.

Fig. 8 displays the C_{de} profiles during 100 cycles of dual-column TVSA operation. The C_{de} ranged from 87.1 to 96.9% with an average of 92.7% reflecting that the C_{de} could reach a high level after dual-column TVSA operation. This is practical for further utilization in industrial and agricultural applications or permanent storage in the ocean, depleted oil/gas reservoirs, or saline formation.

3.4 Heat values of 13X regeneration

Regeneration heat (Q_{regen}, kJ g^{-1}) and sensible heat (ΔH_s, kJ g^{-1}) of spent 13X were measured by DSC and calculated as[30]

$$\text{Heat} = k_0 \times \int_{t_1}^{t_2} \Delta T \mathrm{d}t = k_0 \times \text{peak area} \qquad (2)$$

where k_0 is the calibration constant which was provided by the manufacturer by the known heat fusion of a synthetic sapphire cylinder (=0.8 kJ K^{-1} min^{-1} g^{-1}); t_1 and t_2 are the times at which DSC signal appears and vanishes, respectively; ΔT (K) is the change in temperature with time. Heat values were also expressed in terms of heat input per mole of CO_2 desorption by dividing desorption capacity (q_{de}) measured byTGA.

Fig. 9 exhibits the TG and DSC curves during a rise in temperature of spent 13X from 25 to 140 °C and CO_2 desorption from the spent 13X at 140 °C with N_2 gas. It is apparent that a downward signal (negative heat flow) appeared in the DSC curve which was used to estimate Q_{regen}. The ΔH_s was estimated using the DSC signal during a rise in temperature of 13X from 25 to 140 °C. The heat input required to overcome the endothermic reaction associated with desorbing CO_2 from the spent 13X (desorption heat, ΔH_d) was thus approximated by the difference between Q_{regen} and ΔH_s.[31] These heat values are listed in Table 1.

The specific ΔH_s (0.95 kJ mol^{-1}-CO_2 K^{-1}) of 13X was lower than the specific heat input to raise the 30% MEA mixture to the

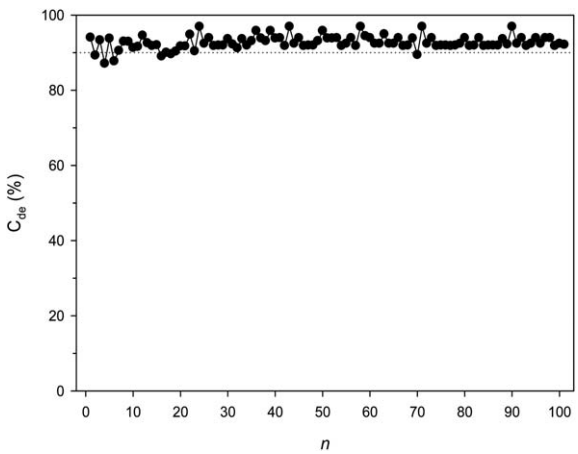

Fig. 8 Peak desorbed CO_2 concentrations during 100 cycles of dual-column TVSA operation.

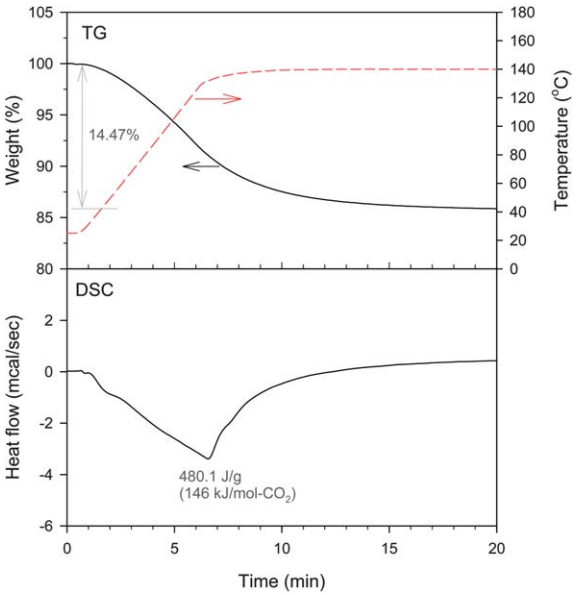

Fig. 9 TG and DSC profiles during a rise in temperature from 25 to 140 °C and desorption of CO_2 from the spent 13X at 140 °C.

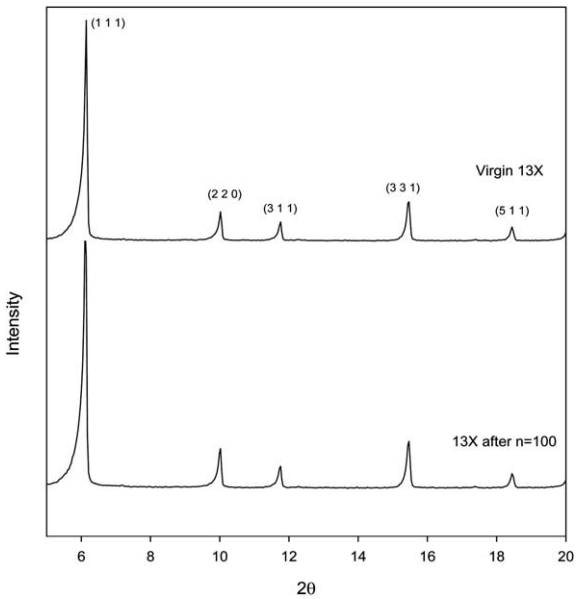

Fig. 10 XRD patterns of 13X before and after 100 cycles of dual-column TVSA operation.

correct temperature for stripping of CO_2 to take place (2.37 kJ mol^{-1}-CO_2 K^{-1}) documented in the literature.[32] The ΔH_d (36.9 kJ mol^{-1}-CO_2), which is very close to the previously reported value (37.44 kJ mol^{-1}-CO_2),[33] also exhibited nearly half the reported value for stripping of CO_2 from the rich CO_2–30% MEA mixture (71.95 kJ mol^{-1}-CO_2).[32] Therefore, if the rise in temperature from the adsorption/absorption process to the desorption process is 115 °C, the heat input required to regenerate spent 13X (122.4 kJ mol^{-1}-CO_2) appears to be much lower than the heat required to regenerate the rich CO_2–30% MEA mixture (344.5 kJ mol^{-1}-CO_2).

3.5 XRD of virgin and regenerated 13X

The crystal phases of 13X after and before 100 cycles of dual-column TVSA operation were characterized by XRD and the results are displayed in Fig. 10. It is evident that these XRD patterns illustrate the characteristics of 13X, which shows a typical peak ($Na_{88}[Si_{104}Al_{88}O_{384}]$) at $2\theta = 6.10°$ (1 1 1).[34] The other diffraction peaks were observed at $2\theta = 10.11°$ (2 2 0), 11.86° (3 1 1), 15.61° (3 3 1) and 18.64° (5 1 1). Both samples have similar XRD patterns reflecting that 13X is a stable material during prolonged dual-column TVSA operation.

3.6 Adsorbent cost of CO_2 capture

Because the pilot-scale test of cyclic CO_2 capture *via* a dual-column TVSA system has not been conducted, it is impossible to estimate capital cost and operational cost at the present time. Capital cost depends on site safety considerations which determines the equipment fee while operational cost relies on site compatibility such as availability of waste heat or streams which determines the regeneration fee. Thus, only the adsorbent cost was considered in the analysis.

The typical price per kilogram of the 13X employed is about US$ 6. The 13X should be reused over thousands of adsorption–desorption cycles to make it a possible cost-effective adsorbent. To evaluate the cost per ton of CO_2 capture of 13X, a statistical analysis based on the best-fit regression of q_w *versus* n in Fig. 7(a) was conducted, and the result is expressed as

$$q_w(n) = 62.6 + 57.09 \times e^{-1.04n} \quad (3)$$

The correlation coefficient (r^2) of above equation is 0.908.

Fig. 11 shows the accumulated amount of CO_2 capture (Q, ton-CO_2/ton-13X) *versus* the corresponding 13X cost of CO_2 capture (US$ per ton-CO_2) through 10^6 cycles of dual-column TVSA operation. The Q at a certain cycle (n) was predicted by summing q_w obtained in eqn (3) from the first to n cycle and multiplying 10^6 while the 13X cost of CO_2 capture at a certain cycle was estimated by dividing 13X cost (US$ 6 per kg of 13X) by the corresponding Q and multiplying 10^3.

The predicted Q and corresponding 13X cost of CO_2 capture at the first cycle of TVSA operation were 0.0831 ton-CO_2 per ton-13X and US$72 386 per ton-$CO_2$. As n reached 1900 and

Table 1 Heat values of 13X regeneration

Desorption heat			Sensible heat		Regeneration heat	
q_{de}/mg g^{-1}	DSC/J g^{-1}	ΔH_d/kJ mol^{-1}-CO_2	DSC/J g^{-1}	ΔH_s/kJ mol^{-1}-CO_2	DSC/J g^{-1}	Q_{regen}/kJ mol^{-1}-CO_2
144.7	121.4	36.9	358.7	109.1	480.1	146.0

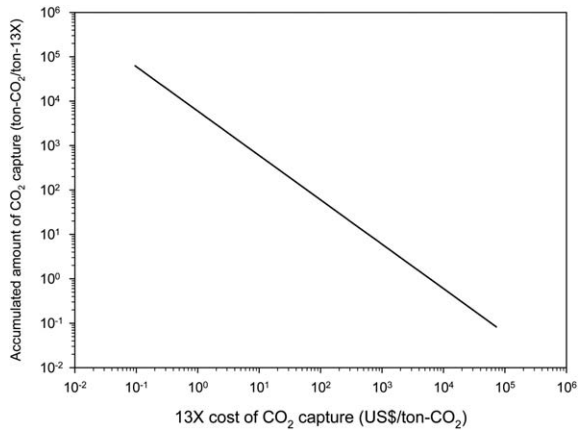

Fig. 11 Cost analysis of 13X for cyclic CO_2 adsorption *via* a dual-column TVSA operation under dry gas stream.

5000, the predicted Q could further increase to 119.6 and 313.8 ton-CO_2 per ton-13X which gave the corresponding 13X cost of US$50 per ton-$CO_2$ and US$19 per ton-$CO_2$, respectively. This reflects the fact that the cost of 13X CO_2 capture could be significantly reduced after extensive dual-column TVSA cycling, and 13X is thus possibly a cost-effective CO_2 adsorbent.

From the foregoing results, the 13X not only displays a high working CO_2 capacity but also is a stable material during 100 cycles of dual-column TVSA operation. The heat input required to regenerate spent 13X was lower than that of a rich CO_2–30% MEA mixture. These advantages make 13X an energy-efficient CO_2 adsorbent. Adsorption with solid 13X *via* a dual-column TVSA operation thus appears a promising CO_2 capture technology.

3.7 Effects of moisture

It must be noted that the cyclic CO_2 adsorption on 13X was performed under dry gas stream, and would be influenced by the presence of moisture in the gas stream.[5] Thus, moisture effects on the CO_2 adsorption of 13X were investigated at 40 and 30 °C *via* a single column system and the results are presented in Fig. 12. The preparation of the humid gas stream is provided elsewhere.[10]

The q_w of 13X at 40 °C were 51.83, 45.89, 42.13, 41.61, 40.12 and 38.85 mg g^{-1} under a relative humidities (RH) of 0, 20.5, 40.9, 61.7, 81.9 and 99.9%, equivalent to water contents in the gas stream of 0, 1.38, 2.75, 4.13, 5.51 and 6.89%, respectively. It is apparent that the q_w of 13X decreased with a rise in RH and showed 25.04% attrition as the RH of the gas stream increased from 0 to 99.9%, which could be explained by the competitive adsorption between CO_2 and H_2O at the same adsorption sites on 13X. The 13X appears moisture-sensitive at 40 °C.

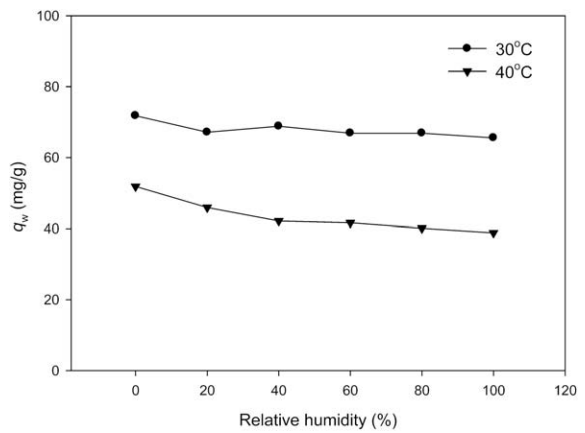

Fig. 12 Effects of RH on 15% CO_2 adsorption on 13X at 30 and 40 °C.

The q_w of 13X at 30 °C were 75.8, 67.1, 68.8, 66.9, 66.1, and 65.5 mg g^{-1} under an RH of 0, 20.5, 40.9, 61.7, 81.9 and 99.9%, equivalent to water contents in the gas stream of 0, 0.82, 1.64, 2.46, 3.28 and 4.10%, respectively. The q_w of 13X showed 11.5% attrition as the RH of gas stream increased from 0 to 20.5%. However, as the RH of the gas stream further increased from 20.5 to 99.9%, no observed changes in q_w were found. This reflects the fact that 13X displays less moisture sensitivity and has a stable adsorption performance of CO_2 under humid conditions below 30 °C. Since the water contents of the gas streams at 25 °C are lower than those at 30 °C, the q_w reported in Fig. 7 would be close regardless of dry or humid conditions.

The typical temperature range of the flue gas in the post flue gas desulfurization system is 45–55 °C, with an average of 50 °C. Therefore, if an adsorption temperature of 25 °C is employed to avoid moisture effects on the CO_2 adsorption of 13X, the temperature of the flue gas must be cooled down from 50 to 25 °C. The enthalpies of the saturated 15% CO_2 gas stream at 50 and 25 °C were 550.02 and 398.57 kJ kg^{-1},[35,36] respectively. The heat released on cooling 1 kg of the saturated 15% CO_2 gas stream from 50 to 25 °C was thus approximated as 151.45 kJ, which could be absorbed by the room-temperature water provided in the field.

4. Conclusions

13X was selected as a CO_2 adsorbent to study cyclic CO_2 capture *via* a dual-column TVSA system. The adsorption capacity and the physical properties of 13X were preserved during 100 cycles of TVSA operation, showing the stability of 13X during extensive TVSA cycling. The desorbed CO_2 concentration level could reach above 90% after TVSA operation, which is practical for further utilization in industrial and agricultural applications or permanent storage in the ocean, depleted oil/gas reservoirs, or saline formation. The low heat input required to regenerate spent 13X helps its prolonged operation and cost effectiveness. The 13X showed less moisture sensitivity and had a stable adsorption performance of CO_2 under humid conditions below 30 °C. These results suggest that a dual-column TVSA system with solid 13X is possibly a promising technology for CO_2 capture from flue gas.

Acknowledgements

Supported from the National Science Council, Taiwan, under Contact NSC99-2221-E-005-032-MY2 is gratefully acknowledged.

References

1 C. M. White, B. R. Strazisar, E. J. Granite, J. S. Hoffman and H. W. Pennline, *J. Air Waste Manage. Assoc.*, 2003, **53**, 645.
2 D. Aaron and C. Tsouris, *Sep. Sci. Technol.*, 2005, **40**, 321.

3 N. MacDowell, N. Florin, A. Buchard, J. Hallett, A. Galindo, G. Jackson, C. S. Adjiman, C. K. Williams, N. Shah and P. Fennell, *Energy Environ. Sci.*, 2010, **3**, 1645.
4 Q. Wang, J. Luo, Z. Zhong and A. Borgna, *Energy Environ. Sci.*, 2011, **4**, 42.
5 A. Sayari, Y. Belmabkhout and R. Serna-Guerrero, *Chem. Eng. J.*, 2011, **171**, 760.
6 E. S. Kikkinides, R. T. Yang and S. H. Cho, *Ind. Eng. Chem. Res.*, 1993, **32**, 2714.
7 M. Radosz, X. Hu, K. Krutkramelis and Y. Shen, *Ind. Eng. Chem. Res.*, 2008, **47**, 3783.
8 T. L. P. Dantas, S. M. Amorim, F. M. T. Luna, I. J. Silva, D. C. S. Azevedo, A. E. Rodrigues and R. F. P. M. Moreira, *Sep. Purif. Technol.*, 2010, **45**, 73.
9 S. Hsu, C. Lu, F. Su, W. Zeng and W. Chen, *Chem. Eng. Sci.*, 2010, **65**, 1354.
10 F. Su, C. Lu and H. S. Chen, *Langmuir*, 2011, **27**, 8090.
11 M. Ishibashi, H. Ota, N. Akutsu, S. Umeda, M. Tajika, J. Izumi, A. Yasutake, T. Kabata and Y. Kageyama, *Energy Convers. Manage.*, 1996, **37**, 929.
12 Y. Takamura, S. Narita, J. Aoki, S. Hironaka and S. Uchida, *Sep. Purif. Technol.*, 2001, **24**, 519.
13 R. V. Siriwardane, M. S. Shen, E. P. Fisher and J. A. Poston, *Energy Fuels*, 2001, **15**, 279.
14 W. K. Choi, T. I. Kwon, Y. K. Yeo, H. Lee, H. Song and B. K. Na, *Korean J. Chem. Eng.*, 2003, **20**, 617.
15 C. T. Chou and C. Y. Chen, *Sep. Purif. Technol.*, 2004, **39**, 51.
16 D. Ko, R. Siriwardane and L. T. Biegler, *Ind. Eng. Chem. Res.*, 2005, **44**, 8084.
17 R. S. Franchi, P. J. E. Harlick and A. Sayari, *Ind. Eng. Chem. Res.*, 2005, **44**, 8007.
18 N. Konduru, P. Lindner and N. M. Assaf-Anid, *AIChE J.*, 2007, **53**, 3137.
19 J. Zhang, P. A. Webley and P. Xiao, *Energy Convers. Manage.*, 2008, **49**, 346.
20 J. Zhang and P. A. Webley, *Environ. Sci. Technol.*, 2008, **42**, 563.
21 J. Merel, M. Clausse and F. Meunier, *Ind. Eng. Chem. Res.*, 2008, **47**, 209.
22 N. Tlili, G. Grévillot and C. Vallières, *Int. J. Greenhouse Gas Control*, 2009, **3**, 519.
23 F. Su, C. Lu, S. C. Kuo and W. Zeng, *Energy Fuels*, 2010, **24**, 1441.
24 C. Lu, F. Su, S. Hsu, W. Chen, H. Bai, J. F. Hwang and H. H. Lee, *Fuel Process. Technol.*, 2009, **90**, 1543.
25 M. G. Plaza, S. García, F. Rubiera, J. J. Pis and C. Pevida, *Chem. Eng. J.*, 2010, **163**, 41.
26 I. M. Smith, CO_2 reduction prospects for coal, *Rep. ICTIS/TR - IEA Coal Res.*, 1999.
27 A. Bosoaga, O. Masek and J. E. Oakey, *Energy Proc.*, 2009, **1**, 133.
28 S. J. Gregg and K. S. W. Sing, *Adsorption, Surface Area and Porosity*, Academic Press, London, 2nd edn, 1982.
29 J. I. Hayashi, M. Yamamoto, K. Kusakabe and S. Morooka, *Ind. Eng. Chem. Res.*, 1997, **36**, 2134.
30 E. Pungor and G. Horvai, *A Practical Guide to Instrumental Analysis*, Boca Raton, FL, CRC-Press, 1994.
31 M. L. Gray, J. S. Hoffman, D. C. Hreha, D. J. Fauth, S. W. Hedges, K. J. Champagne and H. W. Pennline, *Energy Fuels*, 2009, **23**, 4840.
32 G. Gottlicher, *The Energetics of Carbon Dioxide Capture in Power Plants*, U.S. Department of Energy, National Energy Technology Laboratory, 1999.
33 J. Mérel, M. Clausse and F. Meunier, *Environ. Prog.*, 2006, **25**, 327.
34 M. M. J. Treacy and J. B. Hinggins, *Collection of Simulated XRD Powder Patterns for Zeolites, Behalf of the Structure Commission of the International Zeolite Association*, Elsevier, 2001.
35 The Engineering ToolBox; available at, http://www.engineeringtoolbox.com/enthalpy-moist-air-d_683.html.
36 Peace Software, http://www.peacesoftware.de/einigewerte/co2_e.html.